AGU PUBLICATIONS

Geophysical Research Letters

RESEARCH LETTER
10.1002/2014GL061774

Key Points:
- Subtropical connections constrain the variability of tropical biogeochemestry
- A vigorous wind driven-circulation fosters an oxygenated tropical ocean
- Respiration damps the tropical oxygen variability induced by circulation

Supporting Information:
- Figures S1–S3 and Text S1

Correspondence to:
O. Duteil,
oduteil@geomar.de

Citation:
Duteil, O., C. W. Böning, and A. Oschlies (2014), Variability in subtropical-tropical cells drives oxygen levels in the tropical Pacific Ocean, *Geophys. Res. Lett.*, *41*, doi:10.1002/2014GL061774.

Received 8 SEP 2014
Accepted 2 DEC 2014
Accepted article online 4 DEC 2014

Variability in subtropical-tropical cells drives oxygen levels in the tropical Pacific Ocean

Olaf Duteil[1], Claus W. Böning[1], and Andreas Oschlies[1]

[1]GEOMAR Helmholtz Centre for Ocean Research Kiel, Kiel, Germany

Abstract Previous studies found a negative trend in oxygen concentrations in tropical regions during the last decades. Employing a biogeochemical circulation model, we highlight the importance of wind-driven ocean transport associated with the Subtropical-Tropical Cells (STCs) in setting the oxygen levels in the tropical ocean. The observed and simulated slowdown of the STCs by 30% from the 1960s to the 1990s caused a decrease in oxygen transport to the tropics. Transport of phosphate was similarly reduced, decreasing export production and respiration. The effects of physical transport and biological consumption partly compensate, damping oxygen interannual and decadal variability. Our results suggest that the observed residual oxygen trend in the tropical Pacific is mainly driven by changes in oxygen transport. Accordingly, the observed recent strengthening of the STCs leads us to expect a pause in the oxygen decrease or even an increase of tropical Pacific oxygen values in the near future.

1. Introduction

Intense Oxygen Minimum Zones are commonly observed at intermediate depth in the eastern part of the tropical Atlantic and Pacific Oceans [*Karstensen et al*., 2008; *Keeling et al*., 2010]. Observations indicate a strong oxygen decline within these regions during the last 50 years [*Stramma et al*., 2008, 2012]. A change in oxygen levels can result from both changes in circulation and biogeochemistry. Remineralization of sinking organic material consumes oxygen in the ocean interior, while transport tends to resupply oxygen by diffusive [*Gnanadesikan et al*., 2012] or advective [*Duteil et al*., 2014; *Montes et al*., 2014] processes. Natural or anthropogenic changes in ocean circulation and export production therefore potentially lead to changes in oxygen concentrations, which may either cancel or reinforce each other on different time scales. For instance, using a coupled biogeochemical circulation model, *Deutsch et al*. [2011] and *Ito and Deutsch* [2013] suggested that in the north eastern tropical Pacific Ocean the changes in oxygen solubility and respiration due to the El Niño–Southern Oscillation (ENSO) compensate, damping the magnitude of the interior oxygen variability on interannual time scales. On decadal time scales, the integrated variability of biogeochemical and physical processes produces a pronounced oxygen variance, possibly correlated with the Pacific Decadal Oscillation (PDO) [*Deutsch et al*., 2011].

In the eastern tropical North Pacific, local changes in the trade winds appear to play a central role in setting oxygen variability as they control the coastal upwelling, biological productivity, and therefore the amount of respiration occurring in the thermocline [*Deutsch et al*., 2014]. The strength of trade winds, connected with the Walker circulation [*Feng et al*., 2011], also affects the linkage between tropical and extratropical regions via upper ocean meridional transports associated with the Subtropical-Tropical Cells (STCs) [*McCreary and Lu*, 1994; *Schott et al*., 2004]. The STCs transport the ventilated waters from subtropical subduction regions along the thermocline toward the equator, where they are upwelled. In the Pacific Ocean, observations have shown a decline of the strength of these cells by 30% over the period 1953 to 2001 [*Zhang and McPhaden*, 2006]. This multidecadal change can be decomposed into two parts: a STC decrease from the 1960s to the mid-1990s followed by a progressive recovery [*McPhaden and Zhang*, 2004; *Feng et al*., 2011]. Model studies showed that the spin-up and spin-down of the STCs contribute to equatorial sea surface temperature anomalies and vertical shifts of the thermocline [*Kleeman et al*., 1999; *Nonaka et al*., 2002; *Lübbecke et al*., 2008]. As suggested by *McPhaden and Zhang* [2002], long-term changes or fluctuations of the STCs might impact the transport of biogeochemical tracers, i.e., of oxygen and nutrients and could thus exert an effective control on oxygen levels in the tropical ocean.

Here we use a coupled biogeochemical circulation model integrated from 1948 to 2007 to assess the mechanisms, physical and biogeochemical, of changes in tropical Pacific oxygen concentrations. After a

description of the experimental strategy (part 2), we assess the multidecadal trend of the simulated interior oxygen concentration and compare it to observations (part 3). We then investigate the mechanisms of the simulated trends, delineating the impacts of oxygen transport and respiration (part 4), followed by an assessment of the role of the STCs in setting the oxygen concentrations in the eastern tropical Pacific Ocean (part 5).

2. Model Experiments

The ocean model builds on the NEMO3.4 code [*Madec*, 2008]. The configuration used is ORCA05 (see *Duteil et al.* [2014] for a more detailed description) in "offline" mode. The offline circulation is provided by a previous interannual ORCA05 "physics-only" simulation, forced by the Coordinated Ocean-ice Research Experiment (CORE) v2 1948–2007 data set [*Large and Yeager*, 2009]. The biogeochemical model is a six-component Nutrient Phytoplankton Zooplankton Detritus (NPZD)-type model optimized by *Kriest et al.* [2010] in a steady state circulation field derived from the Estimating the Circulation and Climate of the Ocean project against global patterns of observed oxygen and phosphate distributions. Inorganic variables include dissolved oxygen (O_2) and phosphate (PO_4). They are linked through exchanges with the biological variables (phytoplankton, zooplankton, particulate, and dissolved organic matter) by a constant Redfield stoichiometry C:N:P:O_2 of 122:16:1:−170.

A spin-up is first performed using the COREv2 "normal year" forcing. After 1000 years of integration, the tracers reached a quasi equilibrium state in the upper 1000 m (Figure S1 in the supporting information). The modeled oxygen distribution in the interior of the ocean (Figure 1a) is consistent with the patterns of the World Ocean Atlas (WOA) [*Garcia et al.*, 2010], with low levels in the eastern tropical regions and high levels in the subtropics and in the regions of water mass formation. The area of suboxic volume (oxygen lower than 5 mmol m^{-3}) appears, however, larger in the model than in the observations. This is the case in most current models [*Cocco et al.*, 2013] as a possible consequence of model grid resolution, which lack an explicit representation of the equatorial zonal jets [*Getzlaff and Dietze*, 2013; *Duteil et al.*, 2014].

We performed two experiments starting from the previously described spun-up state:

1. BIOVAR: the interanually varying 1948–2007 circulation is applied to all the biogeochemical tracers. This experiment assesses the combined role of oxygen transport and respiration variability on the oxygen field variability.
2. BIOCLIM: the interannually varying 1948–2007 circulation is only applied to the oxygen tracer, while a repeated climatological annual cycle circulation is applied to the other tracers, therefore constraining oxygen consumption to climatology. This experiment isolates the impact of oxygen transport variability on the changes in oxygen concentration.

The first 10 years of the experiments are discarded as the shift from climatological to interannual forcing causes an initial perturbation: the analysis focuses on the period 1958–2007.

3. Oxygen Trends in the Ocean Interior

The observed oxygen trend is characterized by a general decline in oxygen concentrations in tropical regions during the last decades, in particular in the Pacific Ocean [*Stramma et al.*, 2008, 2012]. This decline is shown in Figure 1b using data from the World Ocean Database 2013 (WOD2013) (average 160°W–coast, 10°S–10°N: see the data coverage in Figure S2). The 300 m depth level has been chosen as it is located in the upper thermocline, close to the minimum of oxygen values [*Karstensen et al.*, 2008; *Stramma et al.*, 2008; *Keeling et al.*, 2010]. The mean oxygen concentration decreases by about 5 mmol m^{-3} in this region from 1950 to 2010. We only use the grid boxes (see Figure S2) where data are available during all decades to compute the decadal evolution.

In the experiment BIOCLIM, where the biology and hence the respiration is kept at a climatological annual cycle, the changes in the Pacific oxygen concentration from 1958 to 2007 are particularly pronounced (Figure 1c) and are characterized by a linear decline (Figure 1d). In this basin, the mean oxygen concentration decreases by 5 mmol m^{-3} $decade^{-1}$ between 20°S and 20°N, where oxygen is already low (Figure 1c). Bands of strong negative trends are also found around 20° latitude in both hemispheres at the boundaries between subtropical gyres and tropics. In the gyres, between 20° and 40° latitude, the mean oxygen concentration is almost constant. Changes are weaker by 1 order of magnitude in the Atlantic Ocean compared to the Pacific Ocean. In the Southern Ocean, simulated oxygen increases from 40°E to 160°W and decreases from 160°W to 60°W around 50°S.

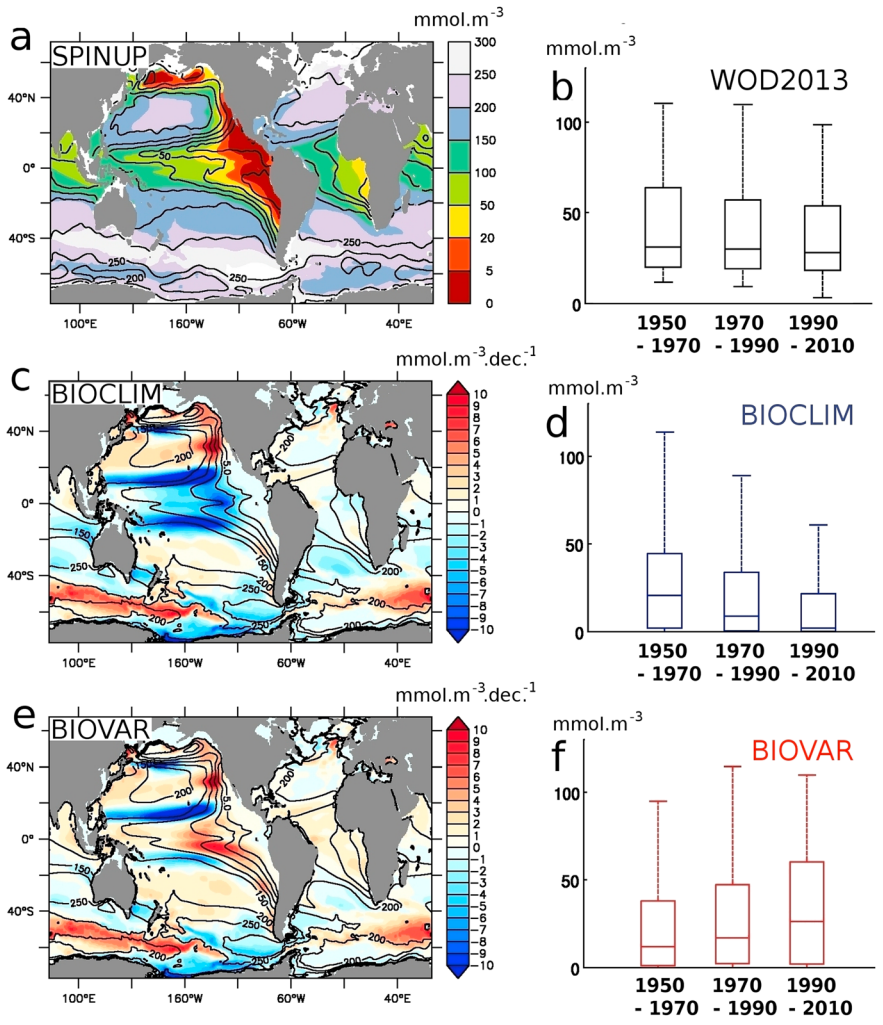

Figure 1. (a) Oxygen concentration (mmol m^{-3}) at 300 m depth after spin-up and from the WOA2013 (contour). (b) Oxygen distribution (160°W:coast, 10°S:10°N) in the WOD2013 observations. Oxygen linear trend (1958–2007) (mmol m^{-3} $decade^{-1}$) and concentration (mmol m^{-3}) after spin-up (contour) at 300 m depth and distribution (160°W:coast, 10°S:10°N) in (c, d) BIOCLIM, (e, f) BIOVAR. Figures 1b, 1d, and 1f are "whisker plots" showing the maximum, first quartile, median, third quartile, and minimum values of the considered data set.

In the experiment BIOVAR (Figures 1e and 1f), where respiration is allowed to vary interannually, the changes in oxygen concentration are strikingly different, especially in the Pacific Ocean. Simulated oxygen concentrations increase linearly by up to 5 mmol m^{-3} $decade^{-1}$ in the central tropical Pacific Ocean, where concentrations below 50 mmol m^{-3} were found in the beginning of the experiment. Overall, the pattern of long-term oxygen change appears closer to observations (Figure 1b) in BIOCLIM (Figure 1d) than in BIOVAR (Figure 1f), suggesting that the biological response might be weaker in reality than in our model. Conversely, the changes in oxygen concentration are similar in BIOCLIM and BIOVAR in the subtropical gyres and the Southern Ocean, showing that in these regions the changes in oxygen concentration are primarily governed by oxygen transport processes, with comparatively minor contributions from biogeochemistry.

4. Mechanisms Leading to Oxygen Changes

4.1. Oxygen Transport (Experiment BIOCLIM)

As seen above, the changes in circulation from 1958 to 2007 are associated with a pronounced oxygen decrease in BIOCLIM, particularly in the tropical Pacific Ocean. This decrease is correlated with a decrease of the strength of the upper tropical meridional overturning circulation (MOC) (Figures 2a and 2b), which

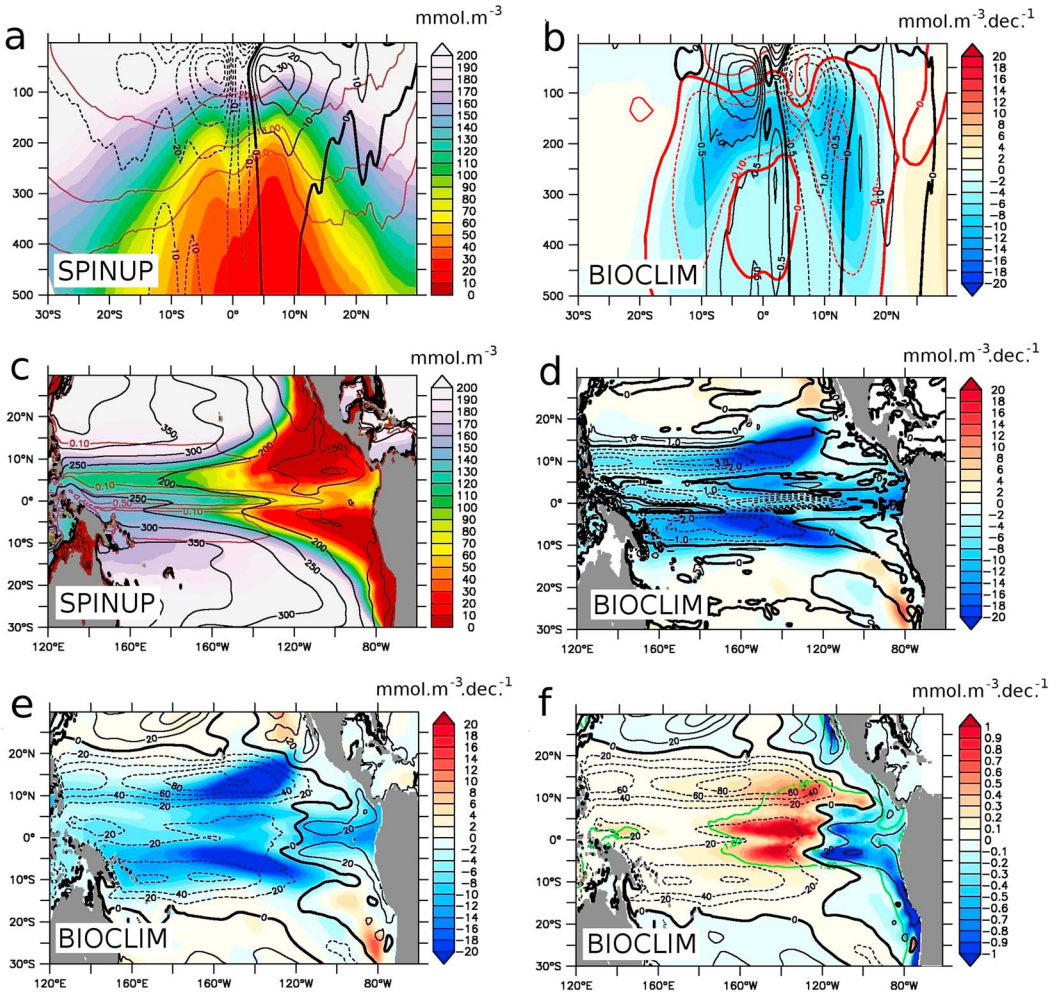

Figure 2. (a) Oxygen concentration (mean 160°W:coast, 10°S:10°N) (mmol m^{-3}) and meridional overturning circulation (contour) (Sv) after spin-up. The isotherms 10°C, 13°C, and 20°C are represented in red. (b) BIOCLIM 1958–2007 oxygen linear trend (mmol m^{-3} $decade^{-1}$), temperature linear trend (°C $decade^{-1}$), and meridional overturning circulation linear trend (Sv $decade^{-1}$). (c) BIOCLIM oxygen concentration at 200 m depth after spin-up (mmol m^{-3}), thermocline (black) (13°C isotherm) depth (m), and absolute velocity (red) (m s^{-1}). (d) BIOCLIM 1958–2007 oxygen concentration linear trend (mmol m^{-3} $decade^{-1}$) and absolute velocity linear trend (m s^{-1} $decade^{-1}$ × 100). (e) BIOCLIM 1958–2007 oxygen concentration linear trend (mmol m^{-3} $decade^{-1}$) and thermocline depth linear trend (m $decade^{-1}$). (f) BIOCLIM 1958–2007 linear trend of respiration (mmol m^{-3} $decade^{-1}$) at thermocline depth (13°C isotherm). Surface phytoplankton concentration (mmolP m^{-3}) is displayed by contour lines.

characterizes the STCs. The simulated 30% multidecadal slowdown of the upper MOC is of the same order of magnitude as deduced from observations [*McPhaden and Zhang*, 2002; *Zhang and McPhaden*, 2006].

The STCs are characterized by a complex three-dimensional circulation. The connection pathway between the subtropical gyres and tropical regions is partly mediated by the equatorial current system, transporting water from the western boundary to the eastern part of the basin. The subsurface tropical circulation (Figure 2c) has been slowing down from 1958 to 2007 (Figure 2d). The modeled equatorial undercurrent velocity maximum at 100°W decreases by 20%, from 0.73 m s^{-1} in the 1950s to 0.58 m s^{-1} in the 2000s. This slowdown is associated with the decrease in the upper meridional overturning. This trend is also manifested in the North and South Equatorial Currents, which constitute the northern/southern limbs of the North/South Pacific Gyres.

The slowdown of the STCs leads to the weakening of the equatorial upwelling and to a flattening of the tropical thermocline, which shallows in the western part and deepens in the eastern part of the basin (Figure 2e). Following *Deutsch et al.* [2011, 2014], the thermocline depth strongly constrains oxygen concentration as it regulates the amount of exported material respired below the mixed layer. While this mechanism is dominant

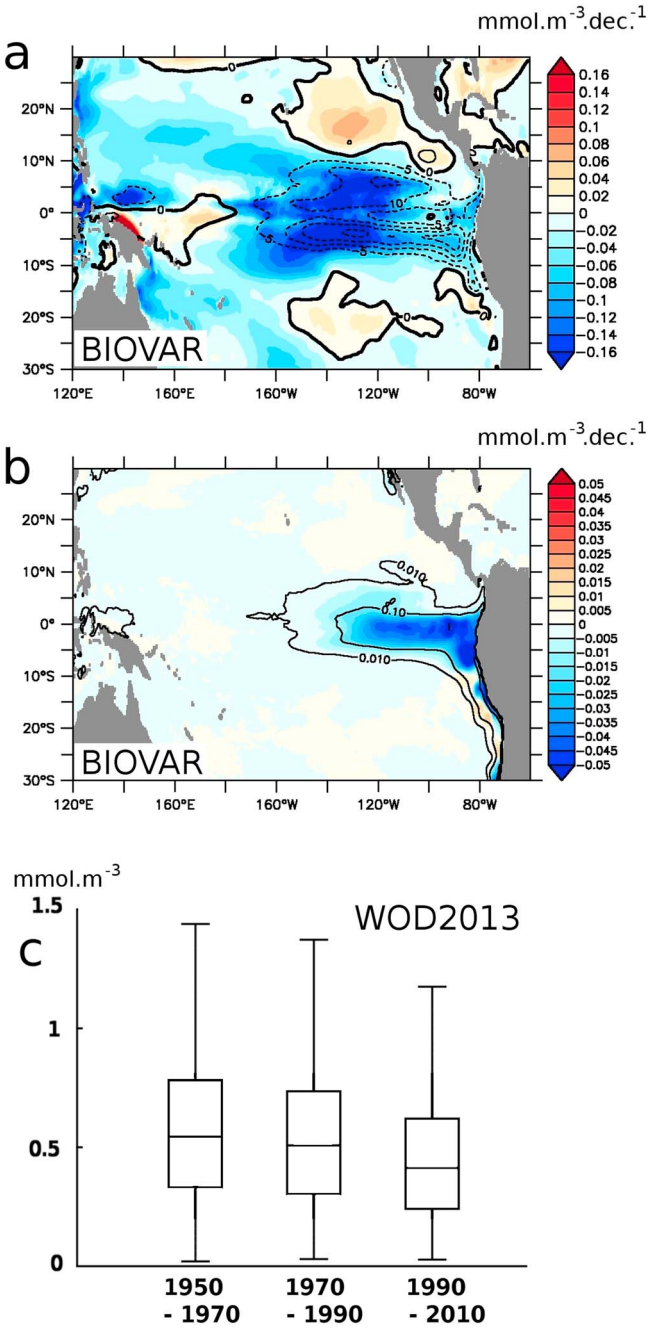

Figure 3. (a) BIOVAR 1958–2007 phytoplankton concentration linear trend (mmolP m^{-2} $decade^{-1}$). The respiration (mmol m^{-3} $decade^{-1}$) linear trend at 300 m is represented in contour. (b) BIOVAR 1958–2007 surface phosphate concentration linear trend (mmol m^{-3} $decade^{-1}$). The phosphate concentration (mmol m^{-3}) after spin-up is represented by contour lines. (c) Surface phosphate concentration (mmol m^{-3}) in the World Ocean Data set 2013 (160°W:coast, 10°S:10°N).

in the eastern boundary upwelling systems poleward of 20° (oxygen concentrations increase as the thermocline deepens), these changes are almost an order of magnitude smaller than the total oxygen changes in the equatorial and tropical regions. The deepening of the eastern equatorial Pacific thermocline is, in fact, associated with an oxygen decrease in experiment BIOCLIM as the impacts of changes in the STC strength and the associated large-scale oxygen supply, such as the advection by equatorial jets, dominate the effects associated with changes in the thermocline depth.

4.2. Oxygen Respiration (Experiment BIOVAR)

Simulated variations of oxygen concentrations in the tropical Pacific thermocline are caused mainly by circulation changes, as seen above, but changes in the oxygen respiration also play some role in our simulations. During the last decades, respiration decreases in the tropics (Figure 3a), due to a reduction of phytoplankton biomass caused by a rarefaction of phosphate in the mixed layer (Figure 3b). The progressive decrease in the strength of the equatorial current system and the STCs has two antagonistic effects: First, a decrease of phosphate supply into the mixed layer, as the equatorial upwelling is reduced. Second, a reduced input of low-phosphate water originating from the gyres, which tends to increase tropical phosphate concentrations. According to our model, the reduction in upwelling dominates and reduces phosphate concentrations in the tropical mixed layer (Figure 3b) and associated export production and respiration. The result is an unrealistic increase in oxygen levels in this region in the BIOVAR experiment despite reduced ventilation (Figure 1d), which is inconsistent with observations (Figure 1b).

While the simulated decline in surface phosphate is in agreement with the WOD2013 data (Figure 3c) (average 160°W–70°W, 10°S–10°N, for data coverage see Figure S3), with a progressive decline by 10% from 1950 to 2010, the model's mean surface phosphate concentration in that area is 1 order of magnitude too low (Figure 3b) due to the neglect of iron limitation in the model. The same surface pattern is shown in

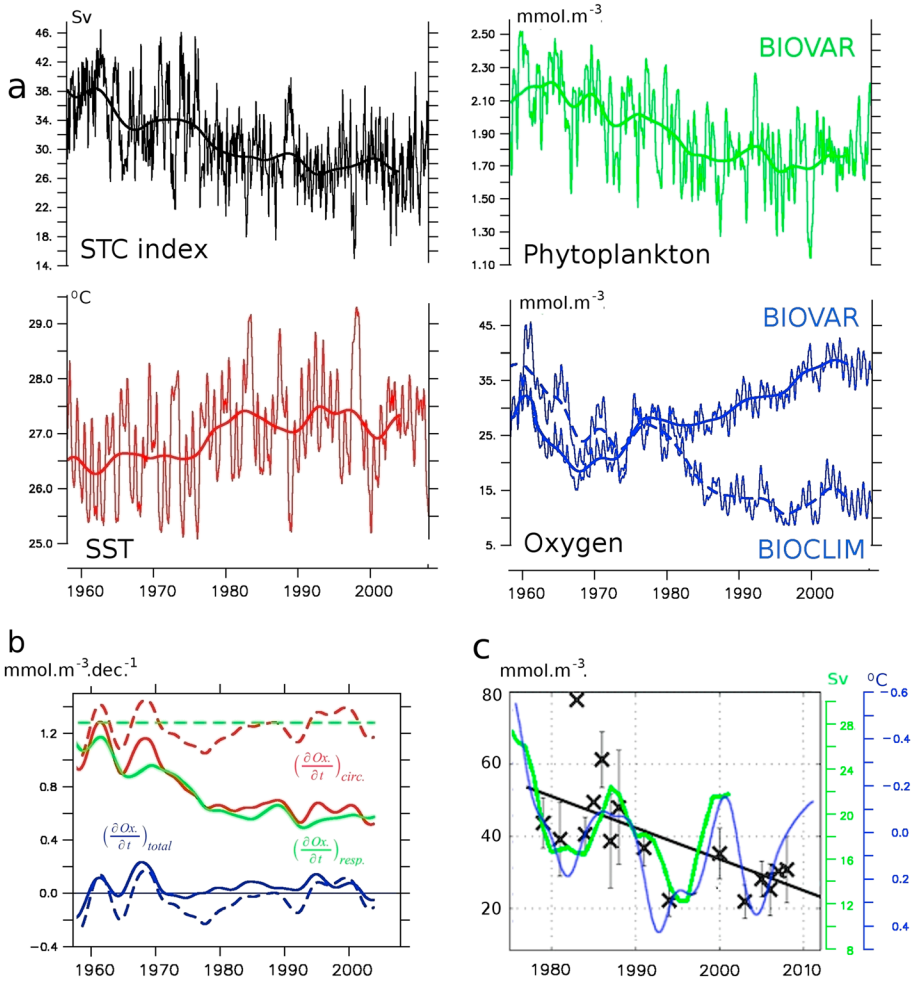

Figure 4. (a) Temporal evolution of the subtropical cell (STC) index (Sv) (black), the sea surface temperature (SST) (degC) (red), the BIOVAR phytoplankton concentration (mmol m^{-2}) (green), the BIOVAR oxygen (plain blue) (mmol m^{-3}), and the BIOCLIM oxygen (dashed blue). The region 160°W:coast, 10°S:10°N is considered. The bold line is the running mean (97 months) of the time series. (b) dO2/d*t* of oxygen in BIOCLIM (dash) and BIOVAR (plain) (mmol m^{-3} $decade^{-1}$). The total dO2/d*t* is represented in blue while dO2/d*t* due to circulation is represented in red and the -dO2/d*t* due to respiration is in green. (c) Symbols show observed oxygen in the eastern Pacific at 110°W (400–700 m). The STC transport inferred from observations by *Zhang and McPhaden* [2006] is plotted in green. The sea surface temperature (SST) anomaly (running mean 97 months) of the eastern Pacific is plotted in blue and is a proxy of the STC variability [*Zhang and McPhaden*, 2006]. The SST data used are from the Hadley Centre SST data set [*Rayner et al.*, 2003]. The figure is adapted from *Czeschel et al.* [2012].

Kriest et al. [2010] from which the biogeochemical model has been adapted (their Figure 4, experiment 28). As that model still yields subsurface oxygen and phosphate concentrations that agree well (and in the RMS metric context agree "best") with observations, we believe that this surface bias does not have substantial effects on our analysis of thermocline oxygen changes.

5. Covariance of Oxygen Concentration and STC Strength

The index of the STC strength has been computed similarly as in *Lohmann and Latif* [2005], as the difference between the maximum and the minimum value of the MOC in the range 10°N–10°S and the upper 250 m of the ocean. The STC index decreases by about 10 Sv from 1960 to 2000 in agreement with previous model studies and observations. In particular, *Lübbecke et al.* [2008] showed a decrease of the same STC index by about 15 Sv from 1958 to 2001 in their reference model configuration. The long-term geostrophic volume transport inferred from observations in the interior ocean pycnocline across 9°N and 9°S decreased by 7 Sv from 1950 (28 Sv) to 2000 (22 Sv) [*Zhang and McPhaden*, 2006].

As a note of caution, the CORE forcing used in the current study may be biased by artificial trends in the wind fields before the mid-1970s, which might lead to an overestimation of the STC decline [*Schott et al*., 2007; *Lübbecke et al*., 2008] and to a damping of decadal variability, which reaches 7–10 Sv in observations [*Zhang and McPhaden*, 2006] while it does not exceed 2–3 Sv in our model experiments. In addition, STC simulations may be affected by spurious model drift possibly reaching 30% of the multidecadal trend [*Feng et al*., 2011]. Removing a drift in the STC transport is not straightforward as biogeochemical processes are characterized by a highly nonlinear behavior. Despite these biases, a lower STC index is nevertheless simulated from 1975 to 2000, corresponding roughly to the positive PDO phase. A recovery of the STCs, correlated with the subsequent negative PDO phase, is simulated during the last years of the model experiment although to a much smaller extent than in observations where the STC strength nearly doubles in a few years [*McPhaden and Zhang*, 2004], from 12 Sv in 1996 to 22 Sv in 2000 [*Zhang and McPhaden*, 2006].

The STC directly impacts tropical subsurface tracers by the STC's advection of anomalies from the midlatitudes [*Gu and Philander*, 1997] and through changes in STC strength and hence the transport of the considered property [*Kleeman et al*., 1999]. As a result, on interannual and decadal time scales the STC index covaries with equatorial sea surface temperatures and phytoplankton concentrations, constrained by the input of nutrients (Figure 4a). Oxygen concentrations vary similarly when the biogeochemical tracers are kept to climatological values (experiment BIOCLIM). In particular, oxygen concentrations in BIOCLIM are characterized by a long-term decrease from 35 to 15 mmol m^{-3} from 1960 to 1995, but tend to stabilize and increase by a few micromoles in the last decade due to the STC recovery. When biology is fully interactive (experiment BIOVAR), the decrease of oxygen consumption compensates the decrease in oxygen transport due to the slower connection with subtropical gyres, ultimately leading to an oxygen increase of about 10 $mmol^{-3}$ during the last 50 years.

The interannual to decadal variability has been estimated by computing the standard deviation of the oxygen time series, after removal of the long-term trend and the application of an 8 year running mean. It is twice as large in BIOCLIM (2.8 mmol m^{-3}) as in BIOVAR (1.4 mmol m^{-3}). The variability in the oxygen concentration is due to both variability in transport and respiration (Figure 4b), which partly compensate in BIOVAR. Such a stabilizing mechanism has been described in ocean models for the upper thermocline of the subpolar north [*Deutsch et al*., 2006] and eastern tropical [*Ito and Deutsch*, 2013] Pacific region. In the latter study the variability of export production and oxygen consumption is, however, strongly constrained as the biological nutrient uptake is parameterized via a linear relaxation of simulated surface nutrients to the respective monthly climatology. Their experiment is therefore intermediate between our model configurations BIOVAR and BIOCLIM. It is characterized by a progressive oxygen decline in the eastern tropical Pacific region from about 40 mmol m^{-3} in 1962 to 10 mmol m^{-3} in 2002 at 300 m depth while year-to-year changes are in the range of a few mmol m^{-3} [see *Ito and Deutsch*, 2013, Figure 2a].

6. Discussion and Conclusion

Using a coupled biogeochemical circulation model, we show that the transport of oxygen from the well-ventilated subtropical gyres to the tropical regions is reduced from 1948 to 2007, leading to a pronounced decrease in oxygen concentrations (about 5 mmol m^{-3} $decade^{-1}$) when respiration is kept at a constant climatological value (experiment BIOCLIM). This study highlights the key role played by the STCs in controlling nutrient and oxygen concentrations in the tropical oceans. The simulated decrease of the strength of these cells by about 30% during the last decades is in good agreement with observations and induces a decline in tropical oxygen concentrations. The variability in biogeochemical and physical processes almost compensates each other and leads to a decreased oxygen variance both on interannual and decadal time scales.

In comparison with observations the long-term oxygen decrease in experiment BIOCLIM, where the biology has been set to a climatological value, is more realistic than the results of experiment BIOVAR, where simulated oxygen levels increase. This suggests that the amplitude of biological changes induced by a slowdown of the upper ocean overturning is weaker in reality than in the model that we employed, possibly due to the lack of iron limitation which in reality regulates the amount of export production. According to our model results, and in contrast to the oxygen changes around 20°N investigated by *Deutsch et al*. [2014], the changes in tropical oxygen concentrations observed during the last decades should be linked mainly to a reduction of oxygen transport.

In a suite of seven Earth system models, *Cocco et al.* [2013] show a mean decrease of oxygen concentration in the upper layer (100–600 m) of the tropical oceans from 1870 to 2100. Similarly, *Bopp et al.* [2013] find an average decrease of oxygen in tropical regions (200–600 m) from 2000 to 2100 in a suite of 10 Coupled Model Intercomparison Project Phase 5 models. While the decrease of primary production (−4 to −10%) driven by enhanced stratification is a robust feature across these models, there is less agreement concerning the evolution of low-oxygen water volume in tropical regions (decrease of 2% to an increase of 16% for a threshold of 50 mmol m^{-3}) presumably due to changes in circulation and in particular in the subtropical cells. *Yang et al.* [2014] showed a large variability in the STC evolution in a subset of 8 CMIP5 models as the long-term trend varies from −2 to +2 Sv from 1900 to 2008 depending of the model considered [*Yang et al.*, 2014].

Our results suggest a close correlation of the strength of the STCs and thermocline oxygen levels in the eastern tropical Pacific. They are thus complementary to the conclusions of *Deutsch et al.* [2011, 2014] who argue that a decrease in trade winds as projected for the next decades would decrease the upwelling strength, leading to a deepening of the thermocline and then an increase in oxygen levels in the eastern tropical North Pacific region. We show that vertical motions of the thermocline have little impact on oxygen concentration in regions where horizontal dynamics and transport are vigorous, in particular close to the equator where a decrease in wind-driven ventilation is associated with a reduction in oxygen levels. For example, *Czeschel et al.* [2012] observed a strong oxygen decrease in the eastern equatorial Pacific (110°W) from the 1980s to the 1990s (50 to 20 mmol m^{-3}) followed by an increase by 20 to 30 mmol m^{-3} from 2000 to 2010. These oxygen variations are consistent with the observed STC variability (Figure 4c), supporting our model-based analysis. Conversely, the modulation of oxygen content in the water column by the variability of the thermocline depth is likely to be more important in regions characterized by strong vertical dynamics, such as the California upwelling system investigated by *Deutsch et al.* [2011, 2014].

In summary, we have shown here that atmospherically driven variations in the STCs connecting tropics and subtropics and controlling oxygen supply to the tropical ocean could explain a large part of the tropical oxygen variability on (multi-)decadal time scales. Future work should focus on analyzing the relationship between large-scale atmospheric forcing patterns and the tropical ocean's oxygenation state in more detail.

Acknowledgments
This work is a contribution of the SFB754 supported by the Deutsche Forschungsgemeinschaft. The model system has been developed as part of the DRAKKAR collaboration. The simulations were performed at the North-German Supercomputing Alliance (HLRN) and the computing centre at Kiel University. The data for this paper are available on request (http://portal.geomar.de/metadata/modelExperiment/show/328810). We thank two anonymous reviewers for their constructive comments.

The Editor thanks two anonymous reviewers for their assistance in evaluating this paper.

References

Bopp, L., et al. (2013), Multiple stressors of ocean ecosystems in the 21st century: Projections with CMIP5 models, *Biogeosciences*, *10*, 6225–6245, doi:10.5194/bg-10-6225-2013, 2013.

Cocco, V., et al. (2013), Oxygen and indicators of stress for marine life in multi-model global warming projections, *Biogeosciences*, *10*, 1849–1868, doi:10.5194/bg-10-1849-2013.

Czeschel, R., L. Stramma, and G. C. Johnson (2012), Oxygen decreases and variability in the eastern equatorial Pacific, *J. Geophys. Res.*, *117*, C11019, doi:10.1029/2012JC008043.

Deutsch, C., S. Emerson, and L. Thompson (2006), Physical-biological interactions in North Pacific oxygen variability, *J. Geophys. Res.*, *111*, C09S90, doi:10.1029/2005JC003179.

Deutsch, C., H. Brix, T. Ito, H. Frenzel, and L. Thompson (2011), Climate-forced variability of ocean hypoxia, *Science*, *333*(6040), 336–339.

Deutsch, C., et al. (2014), Centennial changes in North Pacific anoxia linked to tropical trade winds, *Science*, *345*(6197), 665–668.

Duteil, O., F. U. Schwarzkopf, C. W. Böning, and A. Oschlies (2014), Major role of the equatorial current system in setting oxygen levels in the eastern tropical Atlantic Ocean: A high-resolution model study, *Geophys. Res. Lett.*, *41*, 2033–2040, doi:10.1002/2013GL058888.

Feng, M., C. Böning, A. Biastoch, E. Behrens, E. Weller, and Y. Masumoto (2011), The reversal of the multi-decadal trends of the equatorial Pacific easterly winds, and the Indonesian Throughflow and Leeuwin Current transports, *Geophys. Res. Lett.*, *38*, L11604, doi:10.1029/2011GL047291.

Garcia, H. E., R. A. Locarnini, T. P. Boyer, J. I. Antonov, O. K. Baranova, M. M. Zweng, and D. R. Johnson (2010), World Ocean Atlas 2009, Volume 3: Dissolved oxygen, apparent oxygen utilization, and oxygen saturation, Ed. NOAA Atlas NESDIS 70, 344 pp.

Getzlaff, J., and H. Dietze (2013), Effects of increased isopycnal diffusivity mimicking the unresolved equatorial intermediate current system in an Earth system climate model, *Geophys. Res. Lett.*, *40*, 2166–2170, doi:10.1002/grl.50419.

Gnanadesikan, A., J. P. Dunne, and J. John (2012), Understanding why the volume of suboxic waters does not increase over centuries of global warming in an Earth System Model, *Biogeosciences*, *9*, 1159–1172, doi:10.5194/bg-9-1159-2012.

Gu, D., and S. G. H. Philander (1997), Interdecadal climate fluctuations that depend on exchanges between the tropics and extratropics, *Science*, *275*(5301), 805–807.

Ito, T., and C. Deutsch (2013), Variability of the oxygen minimum zone in the tropical North Pacific during the late twentieth century, *Global Biogeochem. Cycles*, *27*, 1119–1128, doi:10.1002/2013GB004567.

Karstensen, J., L. Stramm, and M. Visbeck (2008), Oxygen minimum zones in the eastern tropical Atlantic and Pacific Oceans, *Prog. Oceanogr.*, *77*, 331–350, doi:10.1016/j.pocean.2007.05.009.

Keeling, R. F., A. Kortzinger, and N. Gruber (2010), Ocean deoxygenation in a warming world, *Ann. Rev. Mar. Sci.*, *2*, 199–229.

Kleeman, R., J. P. McCreary, and B. A. Klinger (1999), A mechanism for generating ENSO decadal variability, *Geophys. Res. Lett.*, *26*, 1743–1746, doi:10.1029/1999GL900352.

Kriest, I., S. Khatiwala, and A. Oschlies (2010), Towards an assessment of simple global marine biogeochemical models of different complexity, *Prog. Oceanogr.*, *86*(3–4), 337–360, doi:10.1016/j.pocean.2010.05.002.

Large, W. G., and S. G. Yeager (2009), The global climatology of an interannually varying air-sea flux data set, *Clim. Dyn.*, *33*(2), 341–364.

Lohmann, K., and M. Latif (2005), Tropical Pacific decadal variability and the subtropical-tropical cells, *J. Clim.*, *18*, 5163–5177.

Lübbecke, J. F., C. W. Böning, and A. Biastoch (2008), Variability in the subtropical-tropical cells and its effect on near-surface temperature of the equatorial Pacific: A model study, *Ocean Sci.*, *4*, 529–569, doi:10.5194/osd-4-529-2007.

Madec, G. (2008), NEMO ocean engine version 3.1. Note Pole Modelisation. 27, Inst. Pierre-Simon Laplace, Paris.

McCreary, J. P., and P. Lu (1994), On the interaction between the subtropical and equatorial ocean circulation: The Subtropical Cell, *J. Phys. Oceanogr.*, *24*, 466–497.

McPhaden, M. J., and D. Zhang (2002), Slowdown of the meridional overturning circulation in the upper Pacific Ocean, *Nature*, *415*, 603–608.

McPhaden, M. J., and D. Zhang (2004), Pacific Ocean circulation rebounds, *Geophys. Res. Lett.*, *31*, L1830, doi:10.1029/2004GL020727.

Montes, I., B. Dewitte, E. Gutknecht, A. Paulmier, I. Dadou, A. Oschlies, and V. Garçon (2014), High-resolution modeling of the Eastern Tropical Pacific oxygen minimum zone: Sensitivity to the tropical oceanic circulation, *J. Geophys. Res. Oceans*, *119*, 5515–5532, doi:10.1002/2014JC009858.

Nonaka, M., S.-P. Xie, and J. P. McCreary (2002), Decadal variations in the subtropical cells and equatorial Pacific SST, *Geophys. Res. Lett.*, *29*(7), 1116, doi:10.1029/2001GL013717.

Rayner, N. A., D. E. Parker, E. B. Horton, C. K. Folland, L. V. Alexander, D. P. Rowell, E. C. Kent, and A. Kaplan (2003), Global analyses of sea surface temperature, sea ice, and night marine air temperature since the late nineteenth century, *J. Geophys. Res.*, *108*(D14), 4407, doi:10.1029/2002JD002670.

Schott, F., J. McCreary, and G. Johnson (2004), Shallow overturning circulations of the tropical-subtropical oceans, in *Earth's Climate: The Ocean-Atmosphere Interaction*, *Geophys. Monogr. Ser.*, vol. 147, edited by C. Wang, S.-P. Xie, and J. A. Carton, pp. 261–304, AGU, Washington, D. C.

Schott, F. A., W. Wang, and D. Stammer (2007), Variability of Pacific subtropical cells in the 50-year ECCO assimilation, *Geophys. Res. Lett.*, *34*, L05604, doi:10.1029/2006GL028478.

Stramma, L., G. C. Johnson, J. Sprintall, and V. Mohrholz (2008), Expanding oxygen-minimum zones in the tropical oceans, *Science*, *320*, 655–658.

Stramma, L., A. Oschlies, and S. Schmidtko (2012), Mismatch between observed and modeled trends in dissolved upper-ocean oxygen over the last 50 yr, *Biogeosciences*, *9*, 4045–4057, doi:10.5194/bg-9-4045-2012.

Yang, C., B. S. Giese, and L. Wu (2014), Ocean dynamics and tropical Pacific climate change in ocean reanalyses and coupled climate models, *J. Geophys. Res. Oceans*, *119*, 7066–7077, doi:10.1002/2014JC009979.

Zhang, D., and M. J. McPhaden (2006), Decadal variability of the shallow Pacific meridional overturning circulation: Relation to tropical sea surface temperatures in observations and climate change models, *Ocean Model.*, *15*, 250–273, doi:10.1016/j.ocemod.2005.12.005.